




RESEARCH PAPER

Expression and role of HIF-1 α and HIF-2 α in tissue regeneration: a study of hypoxia in house gecko tail regeneration

Titta Novianti, ^{a,b} Vetzazah Juniantito,^c Ahmad Aulia Jusuf,^d Evy Ayu Arida,^e Sri Widia A. Jusman,^{f,g} and Mohamad Sadikin^{f,g}

^aDoctoral Program in Biomedical Science, Faculty of Medicine, Universitas Indonesia, Jakarta, Indonesia

^bDepartment of Biotechnology, Universitas Esa Unggul, Jakarta, Indonesia

^cDepartment of Veterinary Clinic Reproduction and Pathology, Faculty of Veterinary Medicine, Agriculture Institute of Bogor, Bogor, Indonesia

^dDepartment of Histology, Faculty of Medicine, Universitas Indonesia, Jakarta, Indonesia

^eIndonesian Institute of Sciences (LIPI) Cibinong, Bogor, Indonesia

^fCenter of Hypoxia and Oxidative Stress Studies (CHOSS), Faculty of Medicine, Universitas Indonesia, Jakarta, Indonesia

^gBiochemistry & Molecular Biology Department, Faculty of Medicine, Universitas Indonesia, Jakarta, Indonesia

ABSTRACT. The house gecko (*Hemidactylus platyurus*) has evolved the ability to autotomize its tail when threatened. The lost part is then regrown via epimorphic regeneration in a process that requires high energy and oxygen levels. Oxygen demand is therefore likely to outstrip supply and this can result in relative hypoxia in the tissues of the regenerating tail. The hypoxic state is stabilized by the Hypoxia Inducible Factor-1 α (HIF-1 α) and HIF-2 α proteins. We induced tail autotomy in 30 mal *H. platyurus*

Correspondence to: Mohamad Sadikin, sadikinmohamad@gmail.com, Center of Hypoxia and Oxidative Stress, Faculty of Medicine, FKUI University of Indonesia, Jakarta Indonesia

Received 2 September 2018; Revised 20 May 2019; Accepted 20 June 2019.

This is an Open Access article distributed under the terms of the Creative Commons Attribution-NonCommercial-NoDerivatives License (<http://creativecommons.org/licenses/by-nc-nd/4.0/>), which permits non-commercial re-use, distribution, and reproduction in any medium, provided the original work is properly cited, and is not altered, transformed, or built upon in any way.

adults using a standard procedure and then collected samples of the regenerated tail tissue on days 1, 3, 5, 8, 10, 13, 17, 21, 25, and 30 post autotomy. For each sample, mRNA expression was analyzed by qPCR, proteins were analyzed using Western Blot tests and immunohistochemistry, and the histological structure was analyzed using Hematoxylin and Eosin staining. On day 1, HIF-1 α mRNA expression increased and the tissue was dominated by leucocyte and erythrocyte cells. HIF-1 α mRNA expression peaked on day 3, at which time some cells were actively proliferating, migrating, and differentiating. At the same time as HIF-1 α expression decreased, HIF-2 α mRNA expression increased, as did overall cellular activity. HIF-2 α expression increased more gradually but was present over a longer period of time than HIF-1 α . We hypothesize that HIF-1 α helps to initially stimulate the tissue regeneration process while HIF-2 α functionally takes over the role of HIF-1 α after HIF-1 α succumbs to the oxygen conditions, but we suspect that both HIF-1 α and HIF-2 α play a role in overcoming the tissue's hypoxic state.

KEYWORDS. differentiation, HIF, house gecko, hypoxia, proliferation

INTRODUCTION

Tissue regeneration processes are important in all organisms, especially when an organism is injured, but organisms have different tissue regeneration abilities.¹ Some amphibians are able to regenerate tails and limbs,² while reptiles, especially lizards, are able to regenerate only their tails, following autotomy, and mammals can regenerate neither tails nor limbs. Reptiles are taxonomically positioned between amphibians and mammals,³ and lizards are more closely related to mammals than other reptiles. Reptiles and mammals are both classified as amniotes, and their embryonic developmental processes are similar.⁴ Lizards' autotomous and regenerative abilities are therefore of particular interest in investigations of the biology of tissue regeneration.

The study of lizard limb regeneration has always been very limited in comparison to regeneration research performed on other vertebrates. Lizards are amniotes with a remarkable ability to regenerate amputated tails.^{3,5} The skeleton and musculature of lizard tails are segmented in a way that reflects embryonic development, but regenerated tails consist of single unsegmented cartilaginous tubes.⁶ Although lizards' regenerative processes have been previously described, the sources and molecular mechanisms underlying the regenerative process remain unclear.^{5,7} The green anole lizard, *Anolis carolinensis*, has emerged as a model organism in which to study lizards' regeneration process. However, while *A. carolinensis* has provided insights in the fields of evolution, population genetics, behavior, and

functional morphology, analyses of its gene expression relating to biological processes, including tail regeneration, have been limited.^{8,9}

The early stage of lizard tail regeneration, around 0–10 days post autotomy, is marked by a wound healing phase. When tissue regrowth attempts to cover the injured area, macrophages activate phagocytosis and consume the apoptotic cells.¹⁰ During days 10–15 post autotomy, the injured area is covered by a new tissue layer, forming a blastema-cone that contains adult stem cells that create new tissue from blood, muscle, adipose, and connective tissue.¹¹ The tail growth phase occurs during days 15–25 post autotomy, when the tissues become more compact and the tail grows longer. Further tissue maturation and scaling occur after day 25 post autotomy.⁵

Vertebrates' tissue regeneration processes vary. Vertebrate tissues contain adult stem cells that play important roles in tissue regeneration, turnover, and homeostasis.^{1,12} Regeneration is a very complex process involving cell division, migration, dedifferentiation, and the transdifferentiation of differentiated cells, all of which contribute to regeneration in several different contexts.¹³ These processes require high energy levels, but since environmental oxygen remains constant at 21% vol. regenerating tissue undergoes a state of relative hypoxia. However, it has been shown that multicellular aerobic organisms are equipped with a mechanism to overcome hypoxic conditions.¹⁴ At the molecular level, aerobic cells have transcription factors that control the expression of genes that can give cells the ability to escape hypoxic conditions. Specifically, two proteins,

Hypoxia Inducible Factors 1 and 2 (HIF-1 and HIF-2), can upregulate the expressions of erythropoietin, vascular endothelium growth factor, glycolytic enzymes, Glutathione, and others enzyme.¹⁵

HIF-1 and HIF-2 is a heterodimer molecule that consists of α and β subunits. The β subunit is an aryl hydrocarbon nuclear translocator and is found in the cell nucleus. HIF-1 β activity is not affected by hypoxic conditions, while the α subunits (HIF-1 α and HIF-2 α) induces adaptation to hypoxic conditions. HIF-1 α also plays a role in oxygen homeostasis. In normoxic conditions, HIF-1 α undergoes hydroxylation at proline residues was produced by HIF-prolyl hydroxylase. Degradation is induced by ubiquitination, and the α subunit is degraded by proteasomes. However, in hypoxic conditions, the hydroxylation process does not occur; instead, HIF-1 α and HIF-2 α migrate into the nucleus and bind to HIF- β to form HIF-1 or HIF-2, which in turn bind to the promoters of target genes.^{16–18}

No description exists in the current literature of the roles played by HIF-1 α and HIF-2 α in the regeneration of whole lizard tails. The aim of the present study was therefore to analyze the expression of HIF-1 α and HIF-2 α during the regeneration of house gecko (*Hemidactylus platyurus*) tails after autotomy. mRNA expression and protein synthesis were analyzed on days 1, 3, 5, 8, 10, 13, 17, 21, 27, and 30 post autotomy.

RESULTS

Growth of H. platyurus tails by length during regeneration

The lengths of regenerating house gecko tails were measured between days 1–30 post autotomy. Tails showed a growth pattern of gradual increase with insignificant changes in length from days 1–13 followed by rapid growth with significant changes in length from days 13–21 and a return to slow growth after day 25 (Fig. 1A). Moreover, there were significant differences in tail length between days 13–17 and also between days 17–21; however, tails were not significantly longer on day 30 than on day 25. Differences between

each group were tested with Kruskal-Wallis. *H. platyurus* tail growth and lengths are shown in Fig. 1B.

Analysis of histological

On day 1, the tail tissue was invaded by leucocyte cells, indicating an inflammation process. Erythrocyte cells typically dominate in tissue injuries, and their presence in the injury site here have I cated that there was bleeding in this area. In the tissue area, some cells proliferated in the basal lamina and migrated to form a new epithelial layer covering the injury site. On day 3, ganglion neuron cells had formed and spread in the dermis tissue, but the tissue was still dominated by leucocyte and erythrocyte cells, and the basal lamina cells had continued to spread and migrate to the epithelial layer. On day 5, the epithelial layer had become thicker, and endothelial cells appeared in the dermis tissue layer. On day 8, the newly regenerated tissue s dominated by fibroblast-like cells and neuronal cells. On day 10, cell aggregation was observed, and the structure of the dermis and epidermis layers was more compact. Some stem cells were found in the aggregated cells, indicating the beginning of the blastemal phase (Fig. 2).

Day 13 marked the beginning of the true regeneration phase. The connective tissue in the dermis layer was denser, and there were some ganglion neuronal cells, new blood vessels, new muscle cells, and new adipose tissue. On days 17 and 21, the dermis and adipose tissues continued to become was denser and more compact. The endothelial cells in the dermis layer grew larger and the basal laminal cells became more active and proliferated, forming an epithelial layer. Fibroblast-like cells continued to spread in the connective tissue. Days 25–30 marked the maturation phase. On day 25, red cells were found in the blood vessels. On day 30, tissue regeneration process continue to morphogenesis process and formed a bulge along the edge of the tail. The dermis and connective tissue layers were again more compact, and the tail's regeneration was marked as being complete (Fig. 3).

FIGURE 1 The growth of *H. platyurus* tails in centimeters (cm). (A) This figure shows box plots of tail growth on days 1, 3, 5, 8, 10, 13, 17, 21, 25, and 30. Tail growth, as measured by length, was insignificant from days 1–13, but tail length grew significantly from days 13–21. Tail length was also significantly different on day 17 than on day 13 and again between days 17–21. (*) denotes significance ($p < 0,05$). Differences were assessed using Kruskal-Wallis ($p < .05$; $n = 30$). (B) Comparison of lizard tail growth on days 1, 3, 5, 8, 10, 13, 17, 21, 25, and 30.

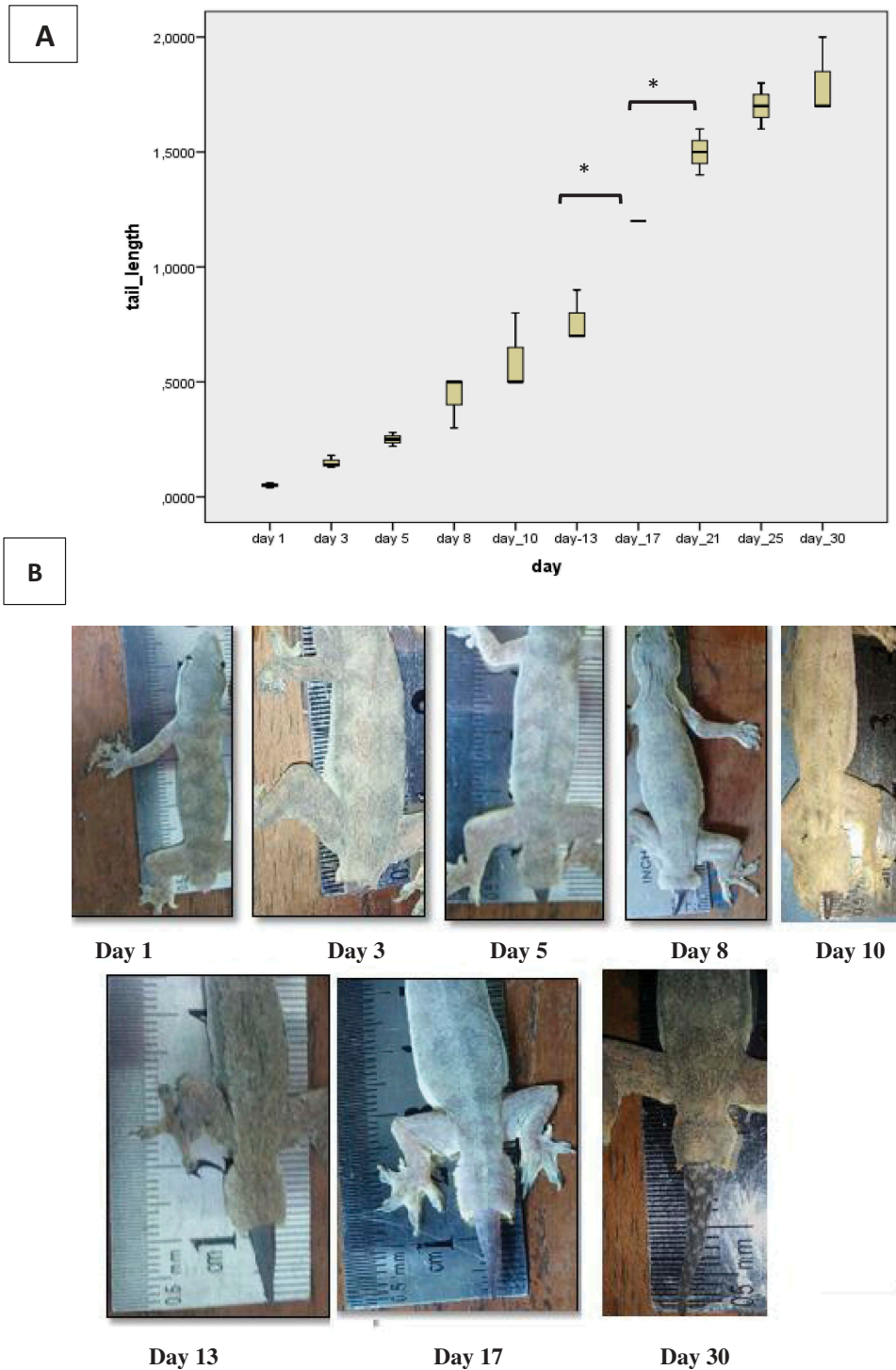
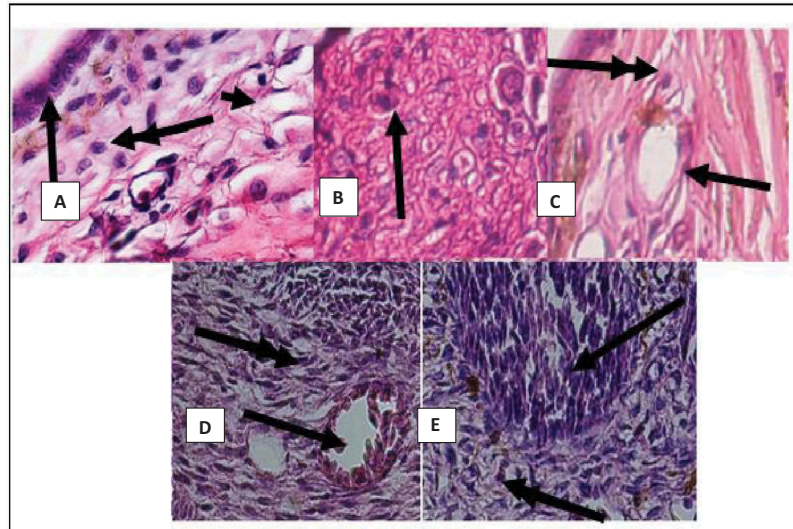


FIGURE 2 Histology of tissue regeneration of *H. platyurus* tails with Hematoxylin-Eosin staining on days 1–10 (40 \times 10 magnification). (A) On day 1, an epithelial layer covered the injury area (single arrow) and the adipose tissue was under a dermis layer (narrow arrow); leucocyte cells (double arrow) were present. (B) On day 3, ganglion cells were observed in the connective tissue (arrow). (C) On day 5, endothelial cells (single arrow) and fibroblast-like cells (double arrow) were observed in the connective tissue. (D) On day 8, fibroblast-like cells spread in the connective tissue (double arrow) and erythrocyte cells were observed in the blood vessels (single arrow). (E) On day 10, aggregated blastemas (single arrow) were present in the dermis layer and contained adult stem cells. Fibroblast-like cells (narrow arrow) and the blood vessels (double arrow) were present in the dermis layer, which was more compact than on day 10.



Analysis of HIF-1 α and HIF-2 α mRNA expressions and proteins using qPCR and western blot tests

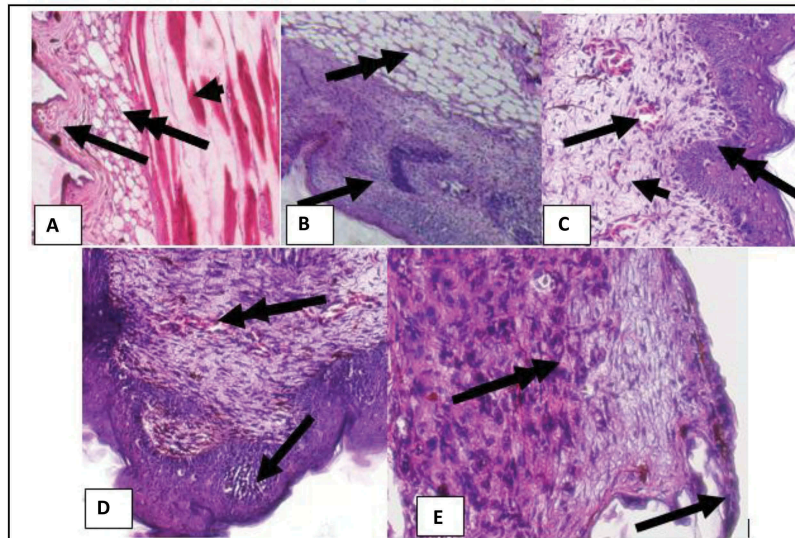
The mRNA expressions of HIF-1 α and HIF-2 α exhibited different patterns, as shown in the box plots in Fig. 4. HIF-1 α mRNA expressions were high on day 1, reached a peak on day 3, and had decreased on day 5; the differences between days 1–3 and 3–5 were both significant. In contrast, HIF-2 α mRNA expressions peaked on day 8 and decreased on day 10, but remained higher than HIF-1 α until day 17. HIF-2 α mRNA expression differed significantly between days 1–3, between days 5–8, and between days 8–10. All differences were assessed using Kruskal-Wallis tests ($p < .05$; $n = 30$).

A curve comparison of the HIF-1 α and HIF-2 α mRNA expressions shows their differences in expression over time. On day 1, HIF-1 α mRNA expression had increased while HIF-2 α mRNA

expression had not. While HIF-1 α mRNA expression peaked on day 3, HIF-2 α mRNA expressed increased more gradually. By day 5, HIF-1 α mRNA expression had begun to decrease, while HIF-2 α mRNA expression began to increase more rapidly until reaching a peak on day 8. Thereafter, HIF-1 α mRNA expression continued to decrease until day 30. HIF-2 α mRNA expression decreased more slowly and remained relatively high until day 17 (Fig. 5).

On the first day, HIF-1 α expression is higher than HIF-2 α . The expression of HIF-1 α reaches its peak on day 3, and continues to decrease until day 5. HIF-2 α expression is relatively slower and longer during tissue regeneration. On day 3, the expression of HIF-1 α and HIF-2 α were relatively high, which indicates that the tissue is in hypoxic state. HIF-2 α expression reaches its peak on day 8 and is able to survive in tissue until day 17, related to its function which plays a role in angiogenesis process.

FIGURE 3 Histology of tissue regeneration of *H. platyurus* tails with Hematoxylin-Eosin staining on days 13–30 (40 x 10 magnification). (A) On day 13, the dermis layer became thicker (single arrow) and there were new adipose (double arrow) and muscle (head arrow) tissues. (B) On day 17, the dermis (single arrow) and adipose (double arrow) tissues were denser and more compact. (C) On day 21, endothelial cells (single arrow) were present in the dermis layer, basal laminal cells (double arrow) were present in the epidermis, and fibroblast-like cells (narrow arrow) were present in the dermis layer. (D) On day 25, the endothelial cells contained red blood cells (double arrow) and the aggregated blastemas were observed in the dermis (single arrow). (E) On day 30, the epidermis formed a bulge along the edge of the tail (single arrow) and the fibroblast-like cells spread within the connective tissue (double arrow).



Western Blot test results showed that HIF-2 α proteins continued to be expressed until day 13, although the band was thin. HIF-1 α proteins appeared on days 1–5 but not on any other days. HIF-2 α proteins appeared on days 1–13 but not on other days. HIF-2 α 's proteins had a molecular weight of 50 KDa, while HIF-1 α proteins weighed 52 KDa. Western Blot tests showed the presence of HIF-1 α proteins until day 5 (Fig. 6).

Table 1 shows the ratio of the band intensities of HIF-1 α and HIF-2 α proteins to β actin, as the positive control, as identified by Western Blot tests. The ratio of HIF-1 α proteins to β actin was high on the first 5 days; the curve pattern was identical to the mRNA expression curve. The HIF-1 α protein curve peaked on day 3, while the HIF-2 α protein curve peaked on day

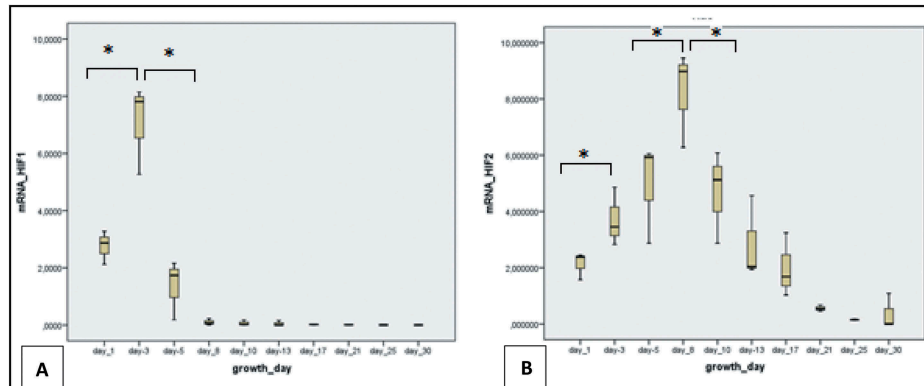
8; its curve patterns were also identical to its mRNA expression curves (Fig. 7).

Immunohistochemistry of HIF-1 α and HIF-2 α

Immunohistochemistry staining showed the distribution of HIF-1 α proteins in the nuclei of basal lamina cells, muscle cells, ganglion neuron cells, and fibroblast-like cells. HIF-1 α proteins were present on days 1–3 (Fig. 8). HIF-2 α proteins appeared on days 1–13 and were distributed in the nuclei of peripheral nerve cells, fibroblast-like cells, and endothelial cells (Fig. 9).

Figure 9. Immunohistochemistry staining of HIF-2 α proteins; magnification is 40 x 10. (A) Mouse liver muscle tissue (positive control). (B)

FIGURE 4 Box plots of HIF-1 α and HIF-2 α mRNA expressions from days 1–30. mRNA expression was quantitatively measured by quantification Polymerase Chain Reaction (qPCR) using the Livak method. All difference tests were conducted using the Kruskal-Wallis method ($p < .05$; $n = 30$); * denotes significance. (A) HIF1- α 's mRNA expression on days 1–30. There were significant differences between days 1–3 and between days 3–5; expression decreased progressively after day 5. (B) HIF2- α mRNA expression on days 1–30. There were significant differences between days 1–3, between days 5–8, and between days 8–10; expression decreased progressively after day 5.



H. platyurus tail tissue regeneration without immunohistochemical staining (negative control). (C) On day 3, HIF-2 α proteins were present in the nuclei of the peripheral nerve (double arrow) and fibroblast-like (single arrow) cells. (D) On day 10, HIF-2 α proteins had spread to the nuclei of the endothelial cells (arrows).

DISCUSSION

Tissue and organ regeneration are important for every organism that experiences an injury.^{1,13} However, higher-orde species have lower regenerative abilities, and lower-order animals must therefore be used to study regeneration. Such regeneration studies typically seek to explore the factors that have important roles in tissue regeneration processes.^{2,19} The choice of a specific animal model is also important. In the present study, we used the house gecko (*H. platyurus*) because it has a high regenerative ability yet is taxonomically closer to mammals than are salamanders or

fish.^{20,21} *H. platyurus* can cast off their tails when threatened, and this autotomy subsequently triggers a tissue regeneration process. *H. platyurus* tails consist of various tissues, including epidermal, dermal, neural, muscle, adipose, bone, and connective tissues.^{22,23}

Tissue and organ regeneration are complex processes involving cells, proteins, and genes.^{5,24} We observed that *H. platyurus* tail regeneration followed a growth curve with three distinct periods. The first 13 days were primarily characterized by wound healing and tail growth was slow. During this period, cells proliferated, differentiated, and migrated, leading to only slight increases in tail length. These findings are consistent with those of Mescher, who found that the beginning of regeneration in mammals consisted of a wound healing phase characterized by proliferation, migration, and differentiation of macrophage, fibroblast, and progenitor cells.²⁵ Similarly, a study of cell migration in zebrafish tissue regeneration reported that progenitor cells and cardiomyocyte cells migrated to the heart tube during

FIGURE 5 Comparison of curves for mRNA HIF-1 α and HIF-2 α expression from day 1–30 in tissue regeneration of *Hemidactylus platyurus* tail.

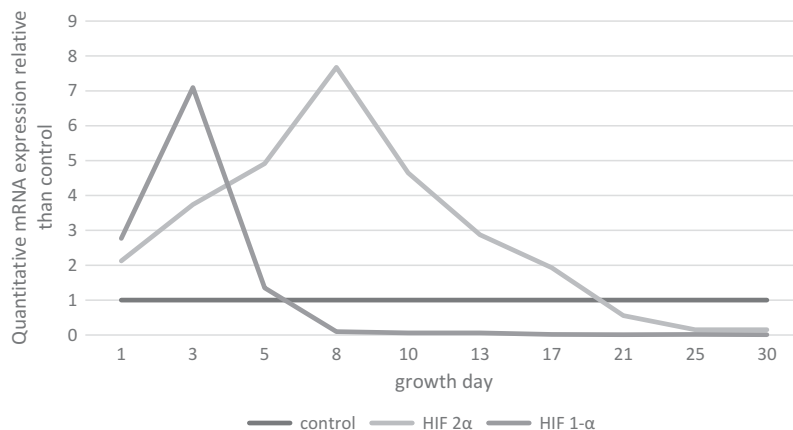


FIGURE 6 Results of Western Blot tests of HIF-1 α , HIF-2 α , and β actin (positive control) proteins from days 1–30. An HIF-1 α protein band appeared only on days 1–5; the molecular weight of these proteins was 52 KDa. An HIF-2 α protein band appeared only on days 1–13; the molecular weight of these proteins was 50 KDa. β actin proteins were also assessed as a positive control; the molecular weight of these proteins was 40 KDa.



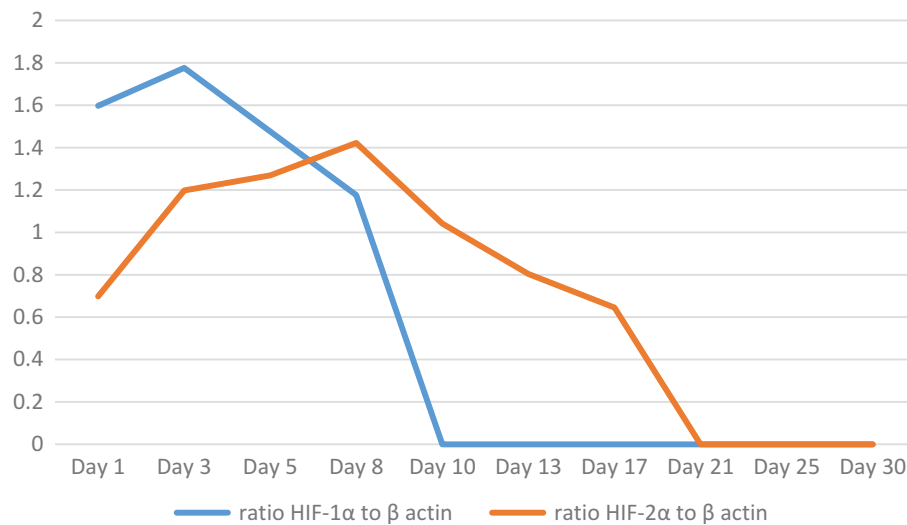
TABLE 1 Band intensities of HIF-1 α , HIF-2 α , and β actin (positive control) proteins on days 1–30, as assessed using Western Blot tests

Sample	Protein band intensity				
	β actin	HIF-1 α	Ratio of HIF-1 α to β actin	HIF-2 α	Ratio of HIF-2 α to β actin
Control	196.042	0	0	0	0
Day 1	177.835	256.149	1.440	214.094	1.203
Day 3	160.442	323.062	2.013	215.818	1.345
Day 5	193.548	225.62	1.165	268.506	1.387
Day 8	214.26	0	0	388.025	1.811
Day 10	230.189	0	0	249.778	1.085
Day 13	212.964	0	0	171.12	0.803
Day 17	192.454	0	0	0	0
Day 21	208.823	0	0	0	0
Day 25	232.781	0	0	0	0
Day 30	213.752	0	0	0	0

TABLE 2 Primer designs for HIF-1 α , HIF-2 α , and 18S genes

Genes		Bases	End product
HIF-1 α	Forward	5' CAG GGC GTG GTA GTA TTC GT 3'	207 bp
	Reverse	5' GAA CCT CCC ATG ACA TGC TT 3'	
HIF-2 α	Forward	5' TCC ATG TTA GGC AAA TGC AA 3'	248 bp
	Reverse	5' ATG AAC ACT GGC CAG GAA AC 3'	
18S	Forward	5' ACA CGC TCC ACC TCA TCT TC 3'	188 bp
	Reverse	5' ATC CCA GAG AAG TTC CAG CA 3'	

FIGURE 7 The ratio curve of HIF-1 α and HIF-2 α to β actin (positive control) proteins on days 1–30 using Western Blot tests. HIF-1 α proteins were high on the first 5 days while HIF-2 α proteins were high on the first 13 days, which corresponded to the entire wound healing phase. HIF-1 α proteins peaked on day 3, while HIF-2 proteins peaked on day 8.



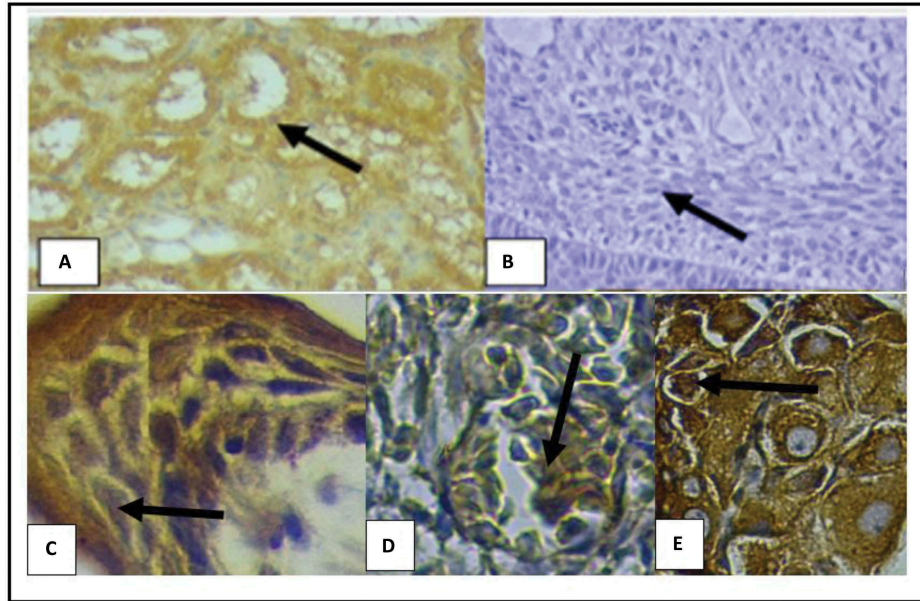
heart tissue regeneration.²⁶ Likewise, another study on the regeneration of house gecko tails found that leukocytes, nerve cells, endothelial cells, and fibroblast-like cells spread throughout the regenerating tissues and that basal lamina cells in the epidermis layer actively proliferated to form an epithelial layer and cover the injury site.¹³

After the wound healing and remodeling phase we observed a tissue regeneration phase, during which tissue growth increased progressively. This was followed by a return to slower growth during a maturation phase, which was histologically characterized by

morphogenesis and tissue maturation. This same pattern of a regeneration phase followed by a maturation phase has been reported in green anole lizard (*A. carolinensis*) tail regeneration.^{8,9}

High cellular activity levels during the wound healing phase require high energy and oxygen levels; however, the atmospheric oxygen supply does not change. As a result, the regeneration process is characterized by a state of relative hypoxia in the regenerating tissues.^{16,17} Gauron et al. also observed that the imbalance between oxygen demand and supply causes regenerating tissue to undergo

FIGURE 8 Immunohistochemistry staining of HIF-1 α proteins; the magnification is 40 \times 10. (A) Mouse renal glomerular tissue (positive control). (B) *H. platyurus* tail tissue regeneration without immunohistochemical staining (negative control). (C) On day 1, HIF-1 α proteins were present only in the nuclei of basal lamina cells (arrow) in the dermis layer. (D) On day 3, they had spread to the nuclei of the fibroblast-like cells (arrow). (E) On day 5, they had spread to the nuclei of the ganglion cells (white arrow).

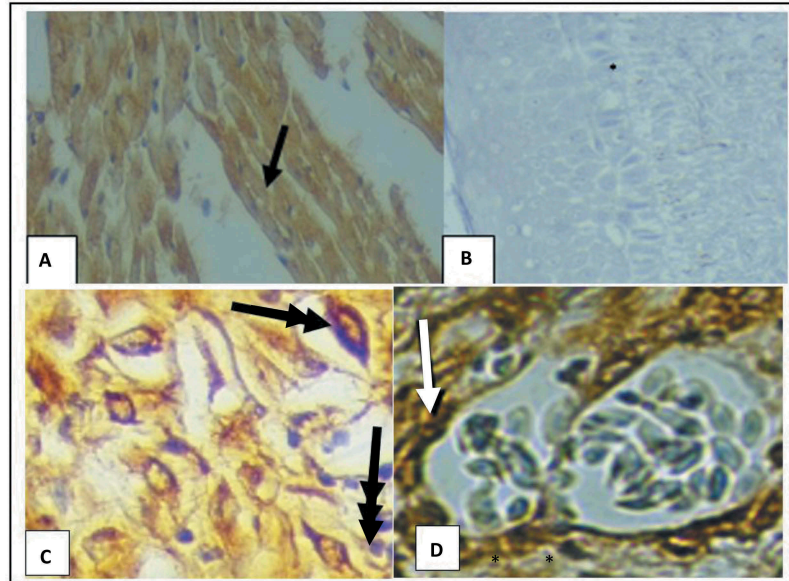


a hypoxic state.²⁷ For example, a study about the role of HIF proteins in zebrafish also found that regenerated tissues experience hypoxia.²⁶ Similarly, both high energy requirements and hypoxia have been indicated in planarian regeneration, as demonstrated, respectively, by cell proliferation and differentiation occurring in close relation with associated high levels of bioenergetics and by an increase of anaerobic glycolysis rates.^{24,28,29}

Generally, regenerating tissue has been shown to respond to hypoxic conditions by producing a transcription factor, HIF, to overcome hypoxia.^{17,30} In the present study, we identified HIF-1 α and HIF-2 α to overcome hypoxia in *H. platyurus* tail regeneration. Both proteins are essentially dimeric (i.e., HIF-1 α and HIF- β for HIF-1, and HIF-2 α and HIF- β for HIF-2) and are constitutive. However, both HIF-1 α and HIF-2 α always degrade in normoxic states and

resynthesize only in hypoxic conditions. In other words, when cellular oxygen levels decrease in regenerating tissue, this inhibits HIF-1 α and HIF-2 α degradation. An hypoxic condition versus *de novo* synthesis of both proteins can be determined by the presence of HIF-1 α and HIF-2 α mRNA.^{15,17,31} However, while it is widely agreed that HIF-1 α and HIF-2 α play critical roles in tissue regeneration and in particular affect cellular response to hypoxic conditions during tissue regeneration, the precise mechanisms and functional effects of HIF-1 α and HIF-2 α remain a source of significant research across a wide variety of species. HIF-1 α , in particular, has received significant research attention.³¹ Weidemann and Johnson reported that HIF-1 α stimulates anaerobic metabolic enzymes, namely glucose transporter proteins and gluconeogenesis enzymes, to increase glucose levels. They further showed that anaerobic

FIGURE 9 Immunohistochemistry staining of HIF-2 α proteins; magnification is 40 x 10. (A) Mouse liver muscle tissue (positive control). (B) *H. platyurus* tail tissue regeneration without immunohistochemical staining (negative control). (C) On day 3, HIF-2 α proteins were present in the nuclei of the peripheral nerve (double arrow) and fibroblast-like (single arrow) cells. (D) On day 10, HIF-2 α proteins had spread to the nuclei of the endothelial cells (arrows).



glucose metabolism was increased by the presence of high levels of lactic acid in the cell; the increased metabolism suggests that HIF-1 α decreases the number of metabolic enzymes that are responsive to oxygen.¹⁷ In a study on the regeneration of amputated distal fingers in mice, Scheerer et al. also found that silencing the HIF-1 α gene in myeloid cells inhibited the regeneration of muscle tissue.³² Halberg et al. further demonstrated the importance of HIF-1 α in the formation of collagen fibers in mouse adipocyte tissue, a synthetic process with high energy needs,³³ while Murdoch et al. found that HIF proteins regulate a number of genes in macrophage cells during hypoxic conditions.³⁴ Semenza and Wang argued that HIF-1 α proteins are able to control erythropoietin synthesis and that the tissue regeneration process was ultimately controlled by HIF-1 α .³⁵ Hu also demonstrated that HIF-1 α plays a role in the proliferation of angiogenesis.³⁶

Against this background, the present study therefore sought to better understand the role

of HIF-1 α in the regeneration of *H. platyurus* tail tissues. We observed an immediate increase in HIF-1 α expression post autotomy, indicating that HIF-1 α is very sensitive to the presence of oxygen. We identified HIF-1 α proteins in basal lamina, leukocyte, nerve, and striated muscle cells during tissue regeneration. We suspected that HIF-1 α regulates several genes that play a role in tissue regeneration, and some evidence for this was provided by the emergence of endothelial cells after peak HIF-1 α expression. Similarly, after HIF-1 α expression decreased, some cells in the regenerating tissue became differentiated and formed new tissue. This suggests that HIF-1 α stimulates genes that affect the regenerative growth of *H. platyurus* tails, as measured by tail length. Our observations of high expressions of HIF-1 α mRNA, as well as of HIF-2 α , also indicated that the regenerating tail tissues were in a hypoxic state. In addition, all of the observed processes confirmed the high energy consumption of the

regeneration process. It seems plausible that the energy required by the regenerating cells is supplied by HIF-1 α proteins stimulating the Erythropoietin enzyme which in turn affects aerobic and anaerobic cellular metabolisms.

Previous research has also implicated a role for HIF-2 α in tissue regeneration and cellular responses to hypoxia during the regeneration process. Hu et al. observed that, in stem cells, HIF-2 α rather than HIF-1 α is needed for the cell's survival in chronic hypoxic conditions.³⁶ Lin et al. reported that HIF-2 α affects the proliferation of zebrafish liver cells during fin tissue regeneration,³⁷ while Patel and Simon asserted that HIF-2 α regulates a number of genes needed for tissue vascularization, including the regulation of peptides and angiogenesis.¹⁸ Koblitz et al. reported the expression of both HIF-1 α and HIF-2 α in zebrafish embryos; as in our study, they found that HIF-2 α appeared later and remained present for longer than HIF-1 α .¹⁶ The relatively longer presence of HIF-2 α suggests an effort to maintain the regulatory process of gene expression in tissues and assure oxygen supply.

Given this previous research, our study sought to characterize the role of HIF-2 α and its relationship to HIF-1 α in *H. platyurus* tail tissue regeneration. We found that there is a certain amount of coordination between HIF-1 α and HIF-2 α : while HIF-1 α reacted earlier than HIF-2 α , HIF-1 α decreased when HIF-2 α began to increase significantly. Expression of HIF-2 α mRNA peaked on day 8, at the same time as endothelial cells and blood vessels spread and formed on the regenerating tissue. We also found HIF-2 α proteins in endothelial, basal lamina, and nerve cells.

HIF-1 α is more sensitive to tissue oxygen content than HIF-2 α , and it is plausible that when tissue oxygen reaches a certain threshold, HIF-2 α increases to functionally replace the role played previously by HIF-1 α . We also observed that after the expression of both HIF-1 α and HIF-2 α decreased, the tissue regeneration process entered to the cell regeneration phase and formed new tissue. In addition, the mRNA expressions and

protein levels of both HIF-1 α and HIF-2 α varied between each observation during days 1–30. This rapid variation indicated that the regenerating tissue actively transcribed genes to produce mRNA and synthesize proteins. Further observations of the *H. platyurus* tail regeneration process showed that the regulation dynamics of HIF-1 α and HIF-2 α expression played important roles in overcoming hypoxia. The tissue's need for oxygen could be fulfilled by either HIF-1 α or HIF-2 α , both of which at different points stimulated the formation of endothelial cells and blood vessels; this suggests that HIF-1 α and HIF-2 α are both important in assuring the supply of oxygen and energy needed to support the tissue regeneration processes.

MATERIALS AND METHODS

Animals

Ethical permission for the research was obtained from the Fakultas Kedokteran Universitas Indonesia (FKUI) Research Ethics Committee (no. 672/UN2.F1/ETIK/VII/2015). We captured 30 male adult house geckos (*H. platyurus*) from the wild. Each gecko weighed 6–8 g and their snout-vents were 115.0 (+/- 6.5) mm long. They were housed together in a single glass box (40 x 20 x 30 cm²) at room temperature, with 12 hours of daylight and 12 hours of dark per 24 hours. The bottom of the box was covered with dried leaves. The geckos were fed flying insects such as mosquitoes and small cockroaches. Water was provided daily in a small bowl. All animals were treated according to Zoology Laboratories Indonesian Institute of Science (LIPI) protocol.

The geckos were stimulated to autotomize their tails using a standard procedure in which slight pressure was applied to area autotomy (1 cm from hemipenis) until the gecko released its tail. They were divided into ten groups of three geckos each, with each group's regenerating tail tissues removed for analysis at different time points. The first group's tail regrowth was removed on day 1 post autotomy, the second group's tail regrowth was removed on day 3

post autotomy, and the others were removed on day 5, day 8, day 10, day 13, day 17, day 21, day 25, and day 30 post autotomy, respectively. The regenerated tail growths were cut at 2.0 cm from each gecko's hemipenis. Each tail sample was divided into two parts: one part was stored at -80°C for mRNA and Western Blot analyses, while the other part was stored in formaldehyde 70% for Hematoxylin and Eosin staining and immunohistochemistry analysis.

Isolation of total RNAs

Total RNAs were isolated and extracted from the regenerated tail tissue using the Master PureTM RNA Purification Kit (Epicentre Illumina Company, www.epibio.com/applications/nucleic-acid...kits/rna.../masterpure-rna-purification-kit). The RNA concentration was determined using a Thermo Scientific varioSCAN Flash microplate reader.

Relative expression of HIF-1 α and HIF-2 α mRNA using qPCR

The expressions of HIF-1 α and HIF-2 α mRNA were measured using qPCR with an Eco48 Illumina machine. We isolated 200 ng of total RNA for 20 μL of qPCR reaction and amplified it to cDNA using qPCR and the KAPA SYBR FAST one-step qPCR universal Kapa Biosystems (KK4650) kit. The 18S gene was used as an internal control.

DNA primers for *H. platyurus* for HIF-1 α and HIF-2 α were not available. We therefore designed a primer using a phylogenetic approach from the house gecko's nearest kin for which primers were available (Table 2). Tracking the geckos' HIF-1 α and HIF-2 α genes was achieved using multiple phylogenetic alignment methods. *Gecko japonicus* was used as a referent for the alignment process, which was conducted using the NCBI BLAST method with multiple alignment methods using the ClustalX technique in Mega7 software. We then selected the basic sequence which had the greatest resemblance to its constituent base. Primary DNA analysis was

performed using Primer3 software (bioinfo.ut.ee/primer3-0.4.0).

The qPCR reaction mixture consisted of 10 μL SYBR Green qPCR reaction mix; 0.2 μL of each forward and reverse primer; 2 μL of the RNA template; 2.4 μL of nuclease-free water; 0.2 μL of 50x Kapa; and 5 μL of 2x Kapa Reverse Transcriptase.

The protocol for the qPCR from Kapa Biosystem (<https://www.sigmaldrich.com/catalog/product/roche/>) was as follows: DNA synthesis at 42°C for 5 minutes; inactivation of Kapa Reverse Transcriptase at 95°C for 5 minutes; 40 cycles at 95°C for 10 seconds; annealing for 30 seconds (57°C for HIF-2 α and 55°C for HIF-1 α); and a 95°C melting curve for 60 seconds. The melting curve was performed to verify the presence of a single amplicon. Non-template control was used as a negative control. The qPCR data were calculated based on the Livak method for PCR¹, with the expression ratio as follows:

$$= 2^{-[\text{Ct}_{\text{target}}(\text{test}) - \text{Ct}_{\text{target}}(\text{calibrator})] - [\text{Ct}_{\text{ref}}(\text{test}) - \text{Ct}_{\text{ref}}(\text{calibrator})]}$$

$$= 2^{-\Delta\Delta\text{Ct}}$$

Quantification was performed by dividing the mean expression value of the hypoxic samples by that of the normoxic samples. The result of that calculation was the number of mRNA expressions that were relatively higher or lower than the control.

Western blot

Whole-tissue lysates were isolated using 1x Ripa lysis buffer. Lysates (50 μg) were resolved on an Sodium Dodecyl Sulphate (SDS) 10% polyacrylamide gel. The tissue samples from the regenerated tails were homogenized with a tissue grinder, followed by centrifugation at 5,000 RPM for 15 minutes. HIF-1 α proteins were detected in the lysate extract using 1:500 anti-HIF-1 α (Rabbit polyclonal, My BioSource, catalog no. MBS241603; [https://www.mybiosource.com/prods/Antibody/Polyclonal/HIF-1 \$\alpha\$ -HIF-1Alpha/HIF-1 \$\alpha\$ /datasheet](https://www.mybiosource.com/prods/Antibody/Polyclonal/HIF-1α-HIF-1Alpha/HIF-1α/datasheet)) and 1:300 anti-HIF-2 α antibody

(Rabbit polyclonal, Novus Biological, catalog no. NB100-122; https://www.novusbio.com/products/hif-2-alpha-epas1-antibody_nb100-122). β actin proteins were used as the positive control at a ratio of 1:4,000 in Phosphate Buffer Saline (PBS) tween solution. The presence of immune complexes indicated the existence of a protein that was detected using common second antibodies: biotinylated anti-rabbit IgG antibody 1:5,000 in PBS tween solution, followed by avidin-HRP 1:10,000 in PBS tween solution. The complexes were revealed by the addition of DAB chromogen (1:10 with buffer). A positive reaction was indicated by the appearance of a black band on the nitrocellulose sheet.

Hematoxylin and eosin staining

The paraffin-embedded samples were sectioned using a microtome and placed on slides. The slices were dewaxed in xylenes and rehydrated using graded alcohols. The slides were incubated in Harris hematoxylin and washed, then incubated again in acid alcohol and ammonia water followed by a wash, and then washed sequentially in ethanol and counterstained with eosin. The slices were then dehydrated using graded alcohols and xylenes and mounted by their cover slide.

Immunohistochemistry

Immunohistochemistry was performed on the paraformaldehyde-fixed, paraffin-embedded samples according to the manufacturer's instructions (My BioSource and LifeSpan BioScience). Rabbit antibody anti-HIF-1 α 1:100 and rabbit antibody anti-HIF-2 α 1:300 were used as the primary antibodies. To bind the primary antibody, 4 drops of Trekkie Universal Link (BioCare Medical; <https://biocare.net/wp-content/uploads/STUHRP700>) were used as a secondary antibody. Horseradish Peroxidase (HRP) streptavidin molecules were used as marker molecules to bind to the secondary antibodies. The HRP molecules were detected by chromogen DAB dye and visualized by imageQuant.

CONCLUSION

HIF-1 α expression occurred earlier than HIF-2 α and also decreased faster because it was more sensitive to the presence of oxygen. HIF-1 α played a role in stimulating the proliferation of various cells in the tissue regeneration process. HIF-2 α continued to increase over a longer period of time than HIF-1 α and took over the functional role HIF-1 α in tissue regeneration. HIF-2 α was able to adapt to chronic hypoxia because of its role in regulating genes involved in angiogenesis and cell proliferation.

ACKNOWLEDGMENTS

We would like to thank to the University of Indonesia for funding this research (Universitas Indonesia (UI) Research Grant no. and Doctoral Final Assignment Grant No. 1314/UN 2.R3.1/HKP.05.00/2018). We would also like to thank Ecosains Company for the chance to use a real-time qPCR Eco machine. Our gratitude is also owed to the Center for Hypoxia and Oxidative Stress in the Biochemistry Department in the Faculty of Medicine at the University of Indonesia and the Indonesian Institute of Sciences (LIPI) for the opportunity to use their laboratory during our research, as well as to the Research Center for Virus and Cancer Biology (PRVKP) at the University of Indonesia. Finally, we would also like to thank the LIPI researchers Dr. Marlina and Dr. Amir, who helped with the design of the *H. platyurus* DNA primer.

FUNDING

This work was supported by the Universitas Indonesia [1314/UN 2.R3.1/HKP.05.00/2018].

ORCID

Titta Novianti  <http://orcid.org/0000-0002-0058-7222>

1. Krafts KP. The hidden drama tissue repair. *Organogenesis*. 2010;6(4):225–33. doi:10.4161/org6.4.12555.
2. Joven A, Simon A. Homeostatic and regenerative neurogenesis in salamanders. *Prog Neurobiol*. March 2018;0–1. doi:10.1016/j.pneurobio.2018.04.006.
3. Lozito TP, Tuan RS. Lizard tail regeneration: regulation of two distinct cartilage regions by Indian hedgehog. *Dev Biol*. 2015;399(2):249–62. doi:10.3389/fbioe.2017.00070.
4. Liu Y, Zhou Q, Wang Y, Luo L, Yang J, Yang L, Liu M, Li Y, Qian T, Zheng Y, et al. Gekko japonicus genome reveals evolution of adhesive toe pads and tail regeneration. *Nat Commun*. 2015;6:1–11. doi:10.1038/ncomms10033.
5. Alibardi L. Morphological and cellular aspects of tail and limb regeneration in lizards. Heidelberg, Germany: Springer; 2010. doi:10.1002/DVDY.24474.
6. Lozito TP, Tuan RS. Lizard tail skeletal regeneration combines aspects of fracture healing and blastema-based regeneration. *Development*. 2016;143(16):2946–57. doi:10.1016/j.ydbio.2014.12.036.
7. Vitulo N, Dalla Valle L, Skobo T, Valle G, Alibardi L. Transcriptome analysis of the regenerating tail vs. the scarring limb in lizard reveals pathways leading to successful vs. unsuccessful organ regeneration in amniotes. *Dev Dyn*. 2017;246(2):116–34. doi:10.1002/DVDY.24474.
8. Ritzman TB, Stroik LK, Julik E, Hutchins ED, Lasku E, Denardo DF, Wilson-Rawls J, Rawls JA, Kusumi K, Fisher RE. The gross anatomy of the original and regenerated tail in the green anole (*Anolis carolinensis*). *Anat Rec*. 2012;295(10):1596–608. doi:10.1002/ar.22524.
9. Fisher RE, Geiger LA, Stroik LK, Hutchins ED, George RM, Denardo DF, Kusumi K, Rawls JA, Wilson-Rawls J. A histological comparison of the original and regenerated tail in the green anole, *Anolis carolinensis*. *Anat Rec Adv Integr Anat Evol Biol*. 2012;295(10):1609–19. doi:10.1002/ar.22537.
10. Hutchins ED, Markov GJ, Eckalbar WL, George RM, King JM, Tokuyama MA, Geiger LA, Emmert N, Ammar MJ, Allen AN, et al. Transcriptomic analysis of tail regeneration in the lizard *Anolis carolinensis* reveals activation of conserved vertebrate developmental and repair mechanisms. *PLoS One*. 2014;9:8. doi:10.1371/journal.pone.0105004.
11. Mescher AL. Macrophages and fibroblasts during inflammation and tissue repair in models of organ regeneration. 2017 March;39–53. doi:10.1002/reg2.77.
12. Nakatani Y, Kawakami A, Kudo A. Cellular and molecular processes of regeneration, with special emphasis on fish fins. *Dev Growth Differ*. 2007;49:145–54. doi:10.1111/j.1440-169X.2007.00917.x.
13. Reinke JM, Sorg H. Wound repair and regeneration. *Eur Surg Res*. 2012;49(1):35–43. doi:10.1159/000339613.
14. Wan C, Gilbert SR, Wang Y, Cao X, Shen X, Ramaswamy G, Jacobsen KA, Alaql ZS, Eberhardt AW, Gerstenfeld LC, et al. Activation of the hypoxia-inducible factor-1 α pathway accelerates bone regeneration. *Proc Natl Acad Sci U S A*. 2008;105(2):686–91. doi:10.1073.pnas.0708474105.
15. Loboda A, Jozkowicz A, Dulak J. HIF-1 versus HIF-2 is one more important than the other? *Vascul Pharmacol*. 2012;56(5–6):245–51. doi:10.1016/j.vph.2012.02.006.
16. Köblitz L, Fiechtner B, Baus K, Lussnig R, Pelster B. Developmental expression and hypoxic induction of hypoxia inducible transcription factors in the zebrafish. *PLoS One*. 2015;10(6):1–15. doi:10.1371/journal.pone.0128938.
17. Weidemann A, Johnson RS. Biology of HIF-1 α . *Cell Death Differ*. 2008;15(4):621–27. doi:10.1038/cdd.2008.
18. Patel SA, Simon MC. Biology of hypoxia-inducible factor-2 α in development and disease. *Cell Death Differ*. 2008;15(4):628–34. doi:10.1038/cdd.2008.
19. Payzin-dogru D, Whited JL. An integrative framework for salamander and mouse limb regeneration. *Int J Dev Biol*. 2018;402:393–402.
20. Bansal R, Karanth KP. Phylogenetic analysis and molecular dating suggest that Hemidactylus anamallensis is not a member of the Hemidactylus radiation and has an ancient late cretaceous origin. *PLoS One*. 2013;8:5. doi:10.1371/journal.pone.0060615.
21. Zug GR, Vindum JV, Koo MS. Burmese Hemidactylus (Reptilia, Squamata, Gekkonidae): taxonomic notes on tropical Asian Hemidactylus. *Sci York*. 2007;58:387–405.
22. Weterings R. Observations of an opportunistic feeding strategy in flat-tailed house geckos (*Hemidactylus platyurus*) living in buildings. *Herpetol Notes*. 2017 March;10:133–35.
23. Tkaczenko GK, Weterings R, Weterings R. Prey preference of the common house geckos *Hemidactylus frenatus* and *Hemidactylus Platyurus*. *Herpetol Notes*. 2014 August;7:483–88.
24. Guedelhofer OC, Alvarado AS. Amputation induces stem cell mobilization to sites of injury during planarian regeneration. *Development*. 2012;139(19):3510–20. doi:10.1242/dev.082099.
25. Mescher AL. Junqueira's basic histology: text & Atlas. [Dany F. -supplied English translation of Histologi Dasar queiraJun]. 12th edn. Jakarta (Indonesia): Penerbit Buku Kedokteran; 2011.
26. Poss KD. Getting to the heart of regeneration in zebrafish. *Semin Cell Dev Biol*. 2007;18(1):36–45. doi:10.1016/j.semcdb.2006.11.009.

27. Gauron C, Rampon C, Bouzaffour M, Ipendey E, Teillon J, Volovitch M, Vríz S. Sustained Production of ros triggers compensatory proliferation and is required for regeneration to proceed. *Sci Rep*. 2013;3:1–9. doi:10.1038/srep02084.
28. Osuma EA, Riggs DW, Gibb AA, Hill BG. High throughput measurement of metabolism in planarians reveals activation of glycolysis during regeneration. *Regeneration*. 2018 August;1–9. doi:10.1002/reg2.95 [Wiley].
29. Pirkmajer S, Filipovic D, Mars T, et al. Hif-1 response to hypoxia is functionally separated from the glucocorticoid stress response in the in vitro regenerating human skeletal muscle. *Am J Physiol Regul Integr Comp Physiol*. 2010; 299: R1693–1700. doi:10.1152/ajpregu.00133.2010
30. Stroka DM, Burkhardt T, Desbaillets I, Wenger RH, Neil DAH, Bauer C, GASSMANN M, CANDINAS D. HIF-1 is expressed in normoxic tissue and displays an organ-specific regulation under systemic hypoxia. *Faseb J*. 2001;15:2445–53. doi:10.1152/ajpregu.00133.2010.
31. Ratcliffe PJ, Ratcliffe PJ. HIF-1 and HIF-2 : working alone or together in hypoxia? *JCI*. 2007;117 (4):862–65. doi:10.1172/JCI31750.
32. Scheerer N, Dehne N, Stockmann C, Swoboda S, Baba HA, Neugebauer A, Johnson RS, Fandrey J. Myeloid hypoxia-inducible factor-1 is essential for skeletal muscle regeneration in mice. *J Immunol*. 2013;191(1):407–14. doi:10.4049/jimmunol.1103779.
33. Halberg N, Khan T, Trujillo ME, Wernstedt-Asterholm I, Attie AD, Sherwani S, Wang ZV, Landskroner-Eiger S, Dineen S, Magalang UJ, et al. Hypoxia-inducible factor 1 induces fibrosis and insulin resistance in white adipose tissue. *Mol Cell Biol*. 2009;29(16):4467–83. doi:10.1128/MCB.00192-09.
34. Murdoch C, Muthana M, Lewis CE. Hypoxia regulates macrophage functions in inflammation. *J Immunol*. 2005;175(10):6257–63. doi:10.4049/jimmunol.175.10.6257.
35. Semenza GL, Wang GL. A nuclear factor induced by hypoxia via de novo protein synthesis binds to the human erythropoietin gene enhancer at a site required for transcriptional activation. *Mol Cell Biol*. 1992;12 (12):5447–54. doi:10.1038/cdd.2008.
36. Hu C, Wang L, Chodosh LA, Keith B, Simon MC. Differential roles of hypoxia-inducible factor 1 alpha (HIF-1 alpha) and HIF-2 alpha in hypoxic gene regulation. *Mol Cell Biol*. 2003;23(24):9361–74. doi:10.1128/MCB.26.9.3514–3526.2006.
37. Lin TY, Chou CF, Chung HY, Chiang CY, Li CH, Wu JL, et al. Hypoxia-inducible factor 2 alpha is essential for hepatic outgrowth and functions via the regulation of leg1 transcription in the zebrafish embryo. *PLoS One*. 2014;9:7.